

# On the magnitude of error in determination of rotation axes

A. Morawiec

Institute of Metallurgy and Materials Science, Polish Academy of Sciences,  
ul. Reymonta 25, 30-59 Kraków, Poland.

E-mail: nmmorawi@cyf-kr.edu.pl  
Tel.: ++48-122952854, Fax: ++48-122952804

## Synopsis

Assuming that errors affecting crystal rotations are random, formulas for the average and maximum errors of rotation axes are provided.

## Abstract

Rotation axes (together with rotation angles) are often used to describe crystal orientations and misorientations, and they are also needed to characterize some properties of crystalline materials. Since experimental orientation data are subject to errors, directions of axes obtained from such data are also inaccurate. A natural question arises: given a resolution of input rotations, what is the average error of the rotation axes? Assuming that rotation data characterized by rotation angle  $\omega$  deviate from actual data by error rotations with fixed angle  $\delta$  but otherwise random, the average error of rotation axes of the data is expressed analytically as a function of  $\omega$  and  $\delta$ . Moreover, a scheme for using this formula in practical cases when rotation errors  $\delta$  follow the von Mises-Fisher distribution is described. Finally, the impact of crystal symmetry on determination of average errors of axis directions is discussed. The presented results are important for assessing the reliability of rotation axes in studies where directions of crystal rotations play a role, e.g. in identifying deformation slip mechanisms.

**Keywords:** crystal orientation; misorientation; rotation axis; crystallographic texture; slip system

August 27, 2024

# 1 Introduction

Various rotation parameterizations are used to describe orientations and misorientations of crystallites. Texture calculations often rely on parameters that are difficult to interpret directly, but in interpersonal communication, orientations and misorientations are usually expressed in terms of easily interpreted rotation axes and rotation angles. A rotation axis consists of points invariant under the rotation. Knowing axis direction may give insight into physics of the process causing the rotation. Directions of rotation axes are explicitly specified to determine some material characteristics. For instance, they are key to establishing slip systems active during plastic deformation or, more generally, to investigating cumulative motions of dislocations leading to macroscopic rotations of crystal lattices. Also, criteria for classifying grain boundaries are based on directions of rotation axes. Some orientation distributions are axial, i.e., crystal orientations are related by rotations about a specific axis. The issue of determining and interpreting rotation axes often appears in studies on crystallographic textures; see, e.g., [1–7].

Experimental orientation data are subject to errors. The magnitudes of errors are characteristic of individual orientation measurement techniques. The orientation resolution typically ranges from hundredths of a degree to several degrees. For standard EBSD orientation mappings, it is usually claimed to be about  $0.5^\circ$ – $1.0^\circ$  [8–10]. Tilting a crystal by several degrees may be needed to detect a change in a TEM spot diffraction pattern. Magnitudes of errors for some non-diffraction techniques can be quite large; the orientation resolution of the metallographic etch-pitting technique is of the order of  $10^\circ$ .

For simplicity, the text below refers to errors affecting single crystal orientation measurements, but it can also be reformulated in terms of features of textures. Orientation data obtained from polycrystalline materials are usually reduced to texture components with component-defining central orientations and some component spreads. The spread of a component can be viewed as a measure of deviations from the central orientation.

The rotation axes obtained from error-affected orientation data are also inaccurate, and inferences based on such axes become uncertain. The question arises about magnitudes of errors in determining axis directions. This problem is the subject of consideration below. A correction is made to the hitherto used expression, originally presented as the formula for the average error in axis direction. In parallel, a formula for the maximum error in axis direction is given. Moreover, a scheme is presented for estimating the average error in axis direction in the case where the rotation errors have the spherical von Mises-Fisher distribution. Since symmetry complicates the determination of axis directions, the opportunity is taken to clarify the issue of the average error in axis direction for rotations representing orientations and misorientations of symmetric crystals.

The remainder of this paper is organized as follows. The next section recalls some basic facts about rotations. Section 3 discusses average deviations of rotation axes for rotation

errors of fixed magnitude. Then, in section 4, the case of distributed magnitudes of rotation errors is briefly considered. The issue of the influence of crystal symmetry on determining the average error of rotation axis is discussed in section 5.

## 2 Basics

Throughout this paper, it is assumed that the crystal point group contains inversion, and considerations are limited to proper rotations. Orientation of a crystal is described by a rotation that transforms a crystal reference frame into an established sample reference frame. The misorientation between two crystals is represented by a rotation that transforms the reference frame of the first crystal into the frame of the second crystal.

Interest in axes of rotations is often associated with research on misorientations between crystals of the same type. The axis and angle of the rotation associated with a misorientation are usually referred to as misorientation axis and misorientation angle, respectively. Misorientation axes are usually specified with respect to the crystal reference frame by indices of their directions.

In the case of orientations, axis directions are important when orientation-dependent changes need to be coupled to external forces, stimuli or constraints. (E.g., for understanding plastic deformation of polycrystals, it is important to know the link between axes of grain rotations and stresses applied to the specimen.) The rotation axes for orientations are frequently specified with respect to the sample reference frame.

As a side note, it is worth mentioning misorientations between crystals of different phases. Interpretation of such misorientations is complicated by the fact that a change of the setting of the crystal coordinate systems in one of the phases, changes the null misorientation, i.e., the latter is not unique. However, as in the case of single phase materials, misorientation axes have a the same fundamental meaning: when one crystal rotates with respect to the other, the axis of rotation is along the direction invariant in both crystals.

With  $\mathbf{k}$  being a unit vector along the rotation axis and  $\omega$  denoting the rotation angle, the pair  $(\mathbf{k}, \omega)$  uniquely identifies the right-hand rotation. It is clear that with  $n$  denoting an integer,  $(\mathbf{k}, \omega)$ ,  $(\mathbf{k}, \omega + 2n\pi)$  and  $(-\mathbf{k}, -\omega + 2n\pi)$  represent the same rotation. To limit these ambiguities, the domain of the rotation parameters needs to be specified. The most convenient, natural and commonly used is the one which consists of rotations closest to the null rotation  $I$  (i.e., the rotation by the angle  $\omega = 0$ ). With this domain, the angles of rotations are non-negative and do not exceed  $\pi$ , and the vectors  $\mathbf{k}$  cover the complete unit sphere. In the case of half-turns, the axes are still ambiguous:  $(\mathbf{k}, \pi)$  and  $(-\mathbf{k}, \pi)$  represent the same rotation. The parameterization by  $(\mathbf{k}, \omega)$  is also singular at the point  $I$ , for which the axis is arbitrary.<sup>1</sup> The point  $I$  corresponds to the case of no rotation and is ignored

---

<sup>1</sup>Some rotation parameterizations are regular at  $I$  (e.g., the parameterization by the rotation vector  $\omega\mathbf{k}$ ). It is known, however, that there is no global singularity-free parameterization of rotations [11], i.e., the pair

here; it is assumed that angles of all rotations are positive, i.e.,  $0 < \omega \leq \pi$ . The choice of the domain of the parameters  $(\mathbf{k}, \omega)$  is essential for the considerations presented below. It is assumed that all analyzed axis/angle parameters are in the described domain.

The deviation  $\beta$  between axes along  $\mathbf{k}$  and  $\mathbf{k}'$  is defined as the angle between these vectors, i.e.,  $\beta = \arccos(\mathbf{k} \cdot \mathbf{k}')$ . Angles appearing in theoretical expressions are in radians, while in practical circumstances, angles are expressed in degrees.

### 3 Axis deviations for rotation errors of given magnitude

Let  $\delta$  denote the angular distance between the measured (i.e., approximate) rotation  $g' \sim (\mathbf{k}', \omega')$  and the true rotation  $g \sim (\mathbf{k}, \omega)$  of an object with no symmetry other than invariance with respect to inversion. With the special orthogonal matrices representing the rotations denoted by the same symbols as the rotations themselves, one has  $\delta = \arccos((\text{Tr}(g'g^{-1}) - 1)/2)$ .

Given a fixed  $\delta$  ( $0 < \delta \leq \pi$ ), the following formal question arises: assuming the error rotations  $g'g^{-1} \sim (\mathbf{h}, \delta)$  have random axes, what is the average of the angle  $\beta$  between the axes of  $g$  and  $g'$ . With vectors  $\mathbf{h}$  uniformly distributed over the unit sphere  $S^2$  (and the remaining parameters fixed), the angle  $\beta$  depends on  $\mathbf{h}$ , i.e.,  $\beta = \beta(\mathbf{h})$ , and the average of  $\beta$  is  $\langle \beta \rangle = \int_{S^2} \beta(\mathbf{h}) d\mathbf{h}$ . Clearly,  $\langle \beta \rangle$  must depend on the rotation angle  $\omega$  of  $g$ . For  $\omega$  near zero, the value of  $\langle \beta \rangle$  is expected to be large. Moreover, when  $g$  is nearly a half-turn, an error may cause a large change of axis direction (Fig. 1).

An analytically derived expression intended to answer the above question was given by Bate et al. [9]. They claim that, on average, the axis of the error-affected rotation is inclined to the true axis by the angle  $\arctan(\delta/\omega)$ . This formula is often referred to in research papers (e.g., [12–19]) and PhD theses (e.g., [20–22]). However, when deriving the above expression, it was incorrectly assumed that the average of  $\beta$  as a function of a variable is equal to the value of the function at the average of the variable. Therefore, the formula of Bate et al. does not represent the angle  $\langle \beta \rangle$ . Moreover, the paper [9] ignores the case of  $\omega \geq \pi - \delta$ .

Assuming the error rotations have random axes, it can be shown (see Appendix A) that with  $\delta < \omega < \pi - \delta$ , the average of  $\beta$  is given by

$$\langle \beta \rangle(\omega, \delta) = \frac{\pi}{2} \frac{\tan(\delta/4)}{\sin(\omega/2)}. \quad (1)$$

There is also a closed-form expression for  $\langle \beta \rangle$  covering the entire range  $0 < \omega \leq \pi$ , but it is much more complex than (1), so it is listed in Appendix A.

Closely related to  $\langle \beta \rangle$  is the maximal angle  $\beta_{\max}$  between axes of the rotations  $g$  and  $g'$ . If  $\delta < \omega < \pi - \delta$ , the maximal deviation is

$$\beta_{\max}(\omega, \delta) = \arccos \left( \sqrt{\frac{\cos \delta - \cos \omega}{1 - \cos \omega}} \right). \quad (2)$$

---

( $\mathbf{k}, \omega$ ) is in this respect no different from other parameterizations.

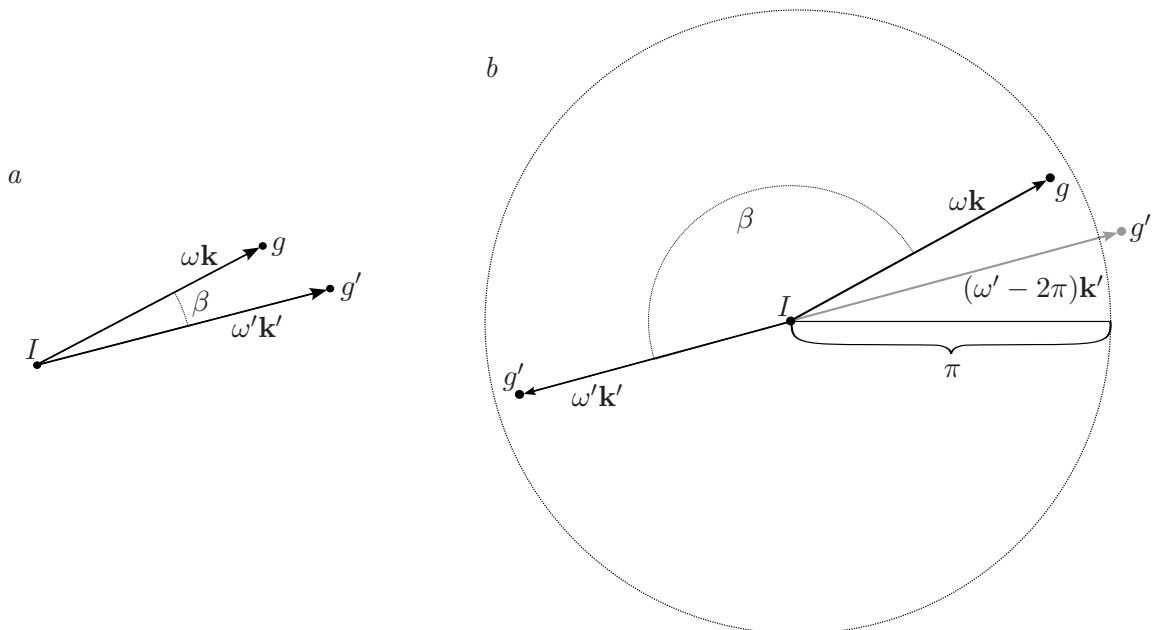


Figure 1: (a) Scheme illustrating definition of the angular deviation  $\beta$  between axes of rotations. The true rotation  $g$  and the deviated rotation  $g'$  are represented by the rotation vectors  $\omega \mathbf{k}$  and  $\omega' \mathbf{k}'$ , respectively. (b) Illustration of the case with  $\omega \geq \pi - \delta$ . The rotation  $g'$  corresponds to  $\omega' \mathbf{k}' = (-\omega')(-\mathbf{k}')$  and to  $(-\omega' + 2\pi)(-\mathbf{k}') = (\omega' - 2\pi)\mathbf{k}'$ , but the latter point is outside the domain adopted for the rotation vectors.

If  $\omega \leq \delta$  or  $\omega \geq \pi - \delta$ , then  $\beta_{\max} = \pi$ . The justification for (2) is provided in Appendix A.

Example plots of the dependence of  $\langle \beta \rangle$  and  $\beta_{\max}$  on  $\omega$  for fixed  $\delta$  ( $= 3^\circ$ ) are shown in Fig. 2. The nature of  $\langle \beta \rangle$  and  $\beta_{\max}$  as functions of  $\omega$  in the domain between 0 and  $\pi$  is better seen in plots for larger  $\delta$ ; an example of such a plot is in Fig. 3. Values of  $\langle \beta \rangle$  and  $\beta_{\max}$  for selected small error magnitudes are listed in Table 1. For other numerical estimates of  $\langle \beta \rangle$  and  $\beta_{\max}$ , see [23, 24].

Clearly, inferences based on axis directions characterized by large  $\langle \beta \rangle$  and  $\beta_{\max}$  must be avoided. Nothing can be done if  $\omega$  is close to 0; in this case, axis directions are unreliable. Data with  $\omega$  close to  $\pi$  can be used by taking into account both the obtained axis direction and the opposite direction.

Before proceeding to the next section, it is worth making the following observation. The above parameter  $\delta$  may characterize orientations or misorientations. However, errors in crystallite misorientations are a consequence of errors in orientation determination. Assuming that 'measured' orientations deviate from (randomly distributed) true orientations by random errors of fixed magnitude  $\delta_o$  ( $0 < \delta_o < \pi/2$ ), the deviations  $\delta_m$  between the error-affected and true misorientations are in the range from 0 to  $2\delta_o$ , and their average equals

$$\langle \delta_m \rangle = \frac{\sin \delta_o - \delta_o \cos \delta_o}{\sin^2(\delta_o/2)}.$$

This expression was derived by analytical averaging over orientations, axes of orientation

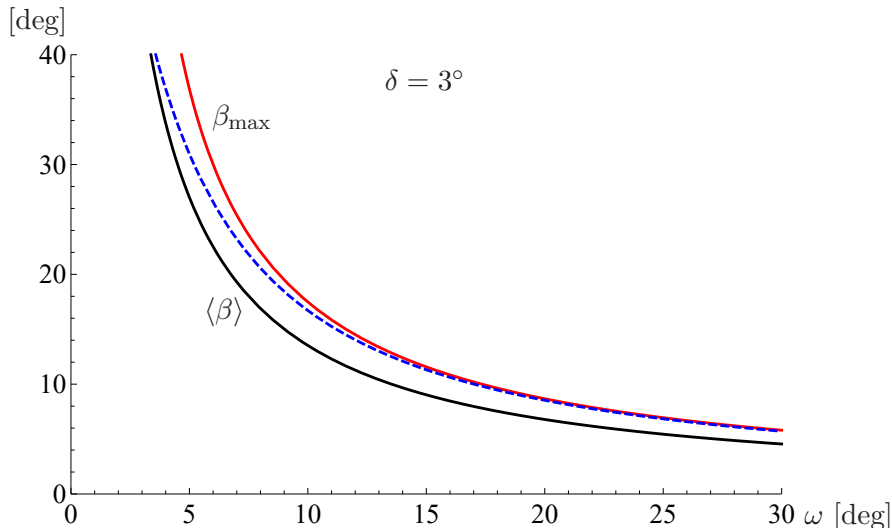


Figure 2: The average  $\langle\beta\rangle$  and maximal  $\beta_{\max}$  angles between axes of the actual and an error-affected rotations versus the rotation angle  $\omega$  for errors of magnitude  $\delta = 3^\circ$ . The dashed blue curve corresponds to the formula of Bate et al. [9].

errors and axes of misorientations. The angle  $\langle\delta_m\rangle$  is well approximated by  $4\delta_o/3$  up to relatively large values of  $\delta_o$ . Thus, in short, if random orientations are affected by errors of small magnitude  $\delta_o$ , then the average error of misorientations has the magnitude of about  $1.333\delta_o$ .

#### 4 Axis deviations for 'randomly' distributed rotation errors

With typical experimental orientation or misorientation data, the magnitude  $\delta$  of the error rotation is not fixed, but it varies, and  $\langle\beta\rangle$  depends on the distribution of  $\delta$ . Given little knowledge of the nature of rotation errors, their distribution must be assumed. If the rotation errors follow the unimodal 'spherically symmetric' von Mises-Fisher distribution [25, 26], their axes are random, and the distribution of their angles  $\delta$  is

$$p(\delta, \hat{\delta}) = N(\hat{\delta}) \left( \frac{\sin(\delta/2)}{\sin(\hat{\delta}/2)} \right)^2 \exp \left( - \left( \frac{\sin(\delta/2)}{\sin(\hat{\delta}/2)} \right)^2 \right), \quad (3)$$

where  $N(\hat{\delta})$  is the normalization coefficient and  $\hat{\delta}$  ( $0 < \hat{\delta} \leq \pi$ ) is the location of the maximum of  $p$ ; see Appendix B. The parameter  $\hat{\delta}$  uniquely determines the shape of  $p$  as a function of  $\delta$ . Example plot of  $p$  versus  $\delta$  is shown in Fig. 4.

With the frequency of occurrence of error magnitudes  $\delta$  described by  $p$ , the  $\omega$ -dependence of the average deviation  $\langle\beta\rangle_p$  between axes of the true and error-affected rotations is

$$\langle\beta\rangle_p(\omega) = \int_0^\pi \langle\beta\rangle(\omega, \delta) p(\delta, \hat{\delta}) d\delta. \quad (4)$$

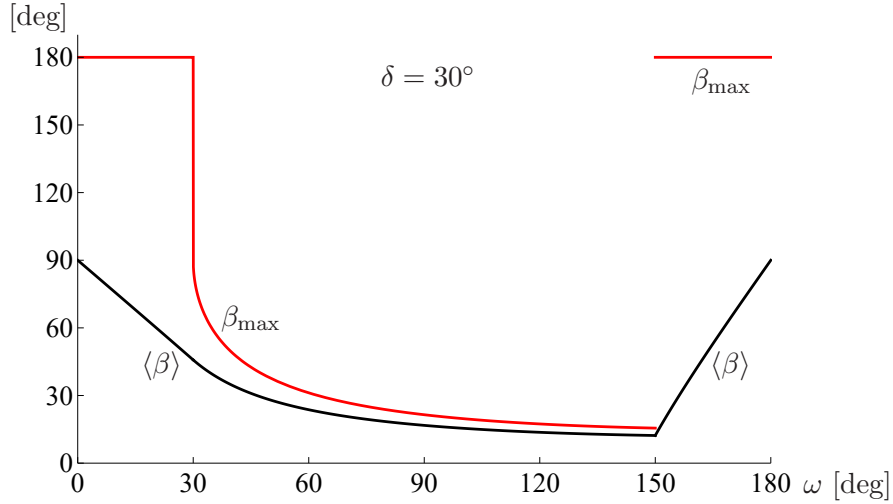


Figure 3: The average  $\langle\beta\rangle$  and maximal  $\beta_{\max}$  angles between axes of the actual and error-affected rotations versus rotation angle  $\omega$  for errors of magnitude  $\delta = 30^\circ$ . The plot of  $\langle\beta\rangle$  for  $0 < \omega \leq \pi$  is drawn using formula listed in Appendix A.

To compute  $\langle\beta\rangle_p(\omega)$  one needs  $\langle\beta\rangle(\omega, \delta)$  expressed by the general formula (7) covering the range  $0 < \delta \leq \pi$ .

The function  $\langle\beta\rangle_p(\omega)$  is uniquely determined by  $\widehat{\delta}$ . Alternatively, the functions  $p$  and  $\langle\beta\rangle_p$  can be specified using the average  $\langle\delta\rangle_p = \int_0^\pi \delta p(\delta, \widehat{\delta}) d\delta$  instead of  $\widehat{\delta}$ . For small  $\widehat{\delta}$ , the angle  $\langle\delta\rangle_p$  is approximately given by  $\langle\delta\rangle_p \approx 1.13 \widehat{\delta}$ . The reason for introducing  $\langle\delta\rangle_p$  is as follows: In cases of interest to orientation-data analyses ( $\langle\delta\rangle_p$  of the order of  $1^\circ$ ), with  $\omega$  sufficiently distant from the ends of its range (say  $2\langle\delta\rangle_p < \omega < \pi - 2\langle\delta\rangle_p$ ), the function  $\langle\beta\rangle_p(\omega)$  is well approximated by  $\langle\beta\rangle(\omega, \langle\delta\rangle_p)$ , i.e., by  $\langle\beta\rangle(\omega, \delta)$  given by (1) with  $\delta$  set at  $\langle\delta\rangle_p$ . Thus, in many practical situations,  $\langle\beta\rangle_p$  can be estimated using the analytical expression (1). Example plots of  $\langle\beta\rangle_p$  versus  $\omega$  are shown in Fig. 5.

Clearly, with rotation errors scattered according to the von Mises-Fisher distribution (i.e., the function that is nowhere equal to zero), the maximal deviation  $\beta_{\max}$  equals  $\pi$ .

$\omega$	$\delta = 0.5$		$\delta = 1.0$		$\delta = 3.0$	
	$\langle\beta\rangle$	$\beta_{\max}$	$\langle\beta\rangle$	$\beta_{\max}$	$\langle\beta\rangle$	$\beta_{\max}$
1.0	22.50	30.00	45.00	180.00	75.00	180.00
2.0	11.25	14.48	22.50	30.00	60.01	180.00
3.0	7.50	9.60	15.00	19.47	45.01	180.00
5.0	4.50	5.74	9.00	11.54	27.01	36.88
7.0	3.22	4.10	6.43	8.22	19.30	25.39
10.0	2.25	2.87	4.51	5.75	13.52	17.48
15.0	1.50	1.92	3.01	3.83	9.03	11.57
30.0	0.76	0.97	1.52	1.93	4.55	5.80
60.0	0.39	0.50	0.79	1.00	2.36	3.00
90.0	0.28	0.35	0.56	0.71	1.67	2.12
150.0	0.20	0.26	0.41	0.52	1.22	1.55
177.0	0.20	0.25	0.39	0.50	1.18	180.00
178.0	0.20	0.25	0.39	0.50	30.93	180.00
179.0	0.20	0.25	0.39	180.00	60.50	180.00

Table 1: Numerical values of average and maximal angles between axes of the actual and error-affected rotations for  $\delta$  equal  $0.5^\circ$ ,  $1.0^\circ$  and  $3.0^\circ$ . All angles are in degrees.

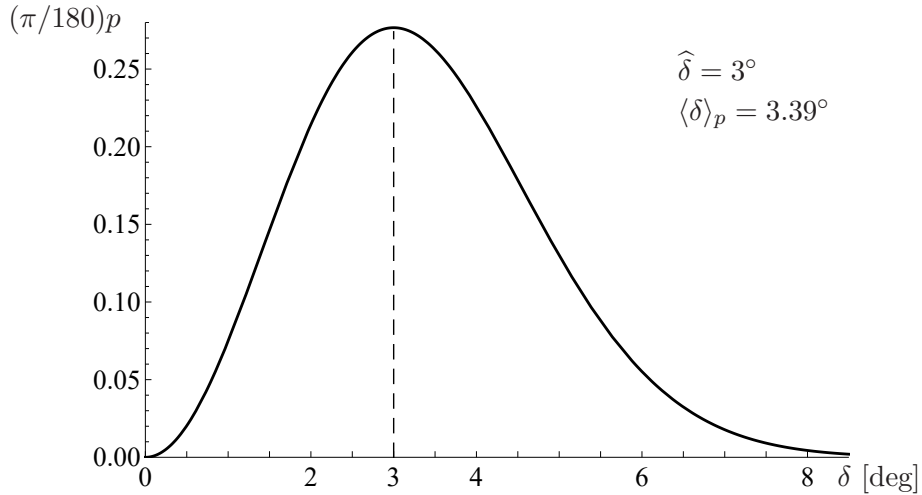


Figure 4: Example distribution  $p$  of rotation angles  $\delta$  for rotation errors following the 'spherical' von Mises-Fisher distribution. The maximum of  $p$  is at  $\delta = 3^\circ$ .

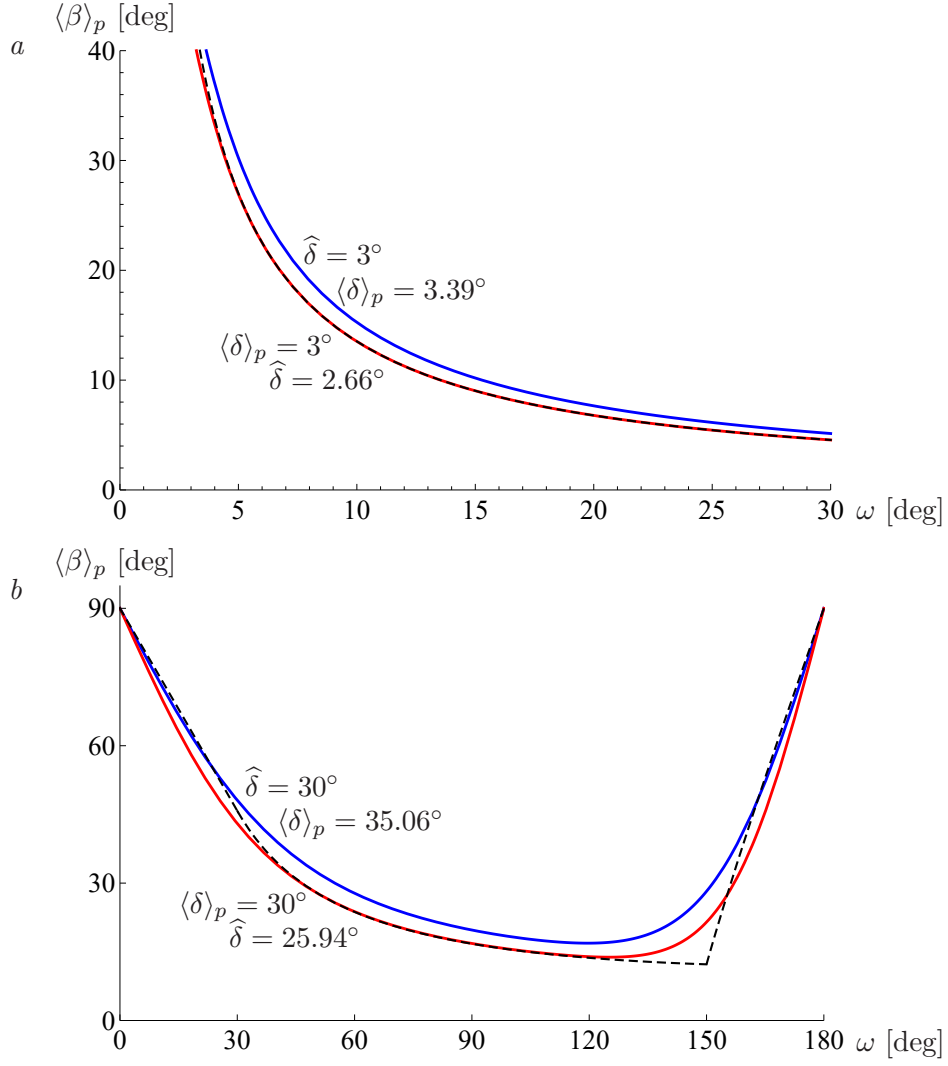


Figure 5: The average angle between axes of the actual and error-affected rotations versus rotation angle  $\omega$  for error magnitudes  $\delta$  distributed as  $p(\delta, \hat{\delta})$  with  $\hat{\delta} = 3^\circ$  (blue) and  $\langle \delta \rangle_p = 3^\circ$  (red) (a) and  $\hat{\delta} = 30^\circ$  (blue) and  $\langle \delta \rangle_p = 30^\circ$  (red) (b). For comparison, the graphs of  $\langle \beta \rangle$  from Figs. 2 and 3 are shown in (a) and (b), respectively, as the dashed black curves.

## 5 Deviations of axes in the case of symmetric objects

The analysis of Bate et al. concerned misorientations between symmetric crystals. However, to account for symmetry, one needs an approach more subtle than that proposed in [9] and followed in section 3 above.

Due to crystal symmetry, distinct but equivalent reference frames can be attached to the crystal, and its orientation can be represented by several different sets of rotation parameters. In some analyzes of symmetric crystals, symmetrically equivalent representations of their orientations are discriminated. For instance, this naturally occurs in dealing with sequences of orientations differing by small-angle rotations: one of symmetrically equivalent crystal reference frames is selected to describe the first orientation of the sequence, and then the same frame is used to describe the subsequent orientations. The choice of the frame in the subsequent orientations relies on the knowledge that the angle of its rotation from the previous one is small. Similarly, positions of the originally selected reference frame can be tracked with known sample rotations; e.g., [1]. However, without such prior knowledge, the choice among equivalent frames is arbitrary. This must be taken into account in determination of rotation axes.

Therefore, one needs to distinguish two cases. The first involves some explicit or tacit assumptions about the rotations which make the choice of crystal reference frames unique. In this case, the symmetry does not play any role, and the approach of section 3 is applicable.

The rest of this section deals with the second case where orientation data are not supplemented with any additional information or assumptions. Symmetric crystals can be assigned reference systems in many equivalent ways. In effect, there are multiple rotations relating reference frames, and rotation parameters are ambiguous. To avoid the ambiguities, rotation parameters are limited to suitably defined domains. This applies to rotations representing both orientations and misorientations. However, certain features of misorientation domains differ from those of orientation domains. Therefore, orientations and misorientations are considered separately.

### *Orientations*

To reduce the arbitrariness in the choice of orientation parameters, data are placed in the so-called fundamental region (FR) such that each internal point of the region represents only one orientation, and points at the boundary of the region have some equivalent points (also at the boundary).<sup>2</sup> FRs for orientations can be obtained by Voronoi tessellation of the rotation space based on points representing (proper) rotations of the crystal point group [27–30]. A convenient choice for FR is the canonical region which contains only representations closest to the null rotation  $I$ , i.e., the region is the Voronoi cell based on  $I$ . Clearly, this definition of FR encompasses the domain for rotations described in section 2.

---

<sup>2</sup>Formally, FR is a closure of a simply connected domain containing exactly one representative of each equivalence class.

Let all measured orientation data be in the  $I$ -based FR, and let  $\omega_0$  be the angular distance from the point  $I$  to the boundary of the FR, i.e., to a boundary point closest to  $I$ . For  $\delta$  and  $\omega$  small compared to  $\omega_0$ , the character of both  $\langle\beta\rangle(\omega, \delta)$  and  $\beta_{\max}(\omega, \delta)$  is the same as that without symmetry. When  $\omega$  exceeds  $\omega_0 - \delta$ , the error may move a rotation from the  $I$ -based Voronoi cell to another cell. In this case, its equivalent in FR has a highly deviating axis. Hence, with  $\omega > \omega_0 - \delta$ , the angle  $\beta$  may become large.

Unlike the case without proper symmetry (section 3), in which the average and the maximal values of  $\beta$  are independent of the rotation axis  $\mathbf{k}$ , in the presence of symmetries, they depend on  $\mathbf{k}$  if  $\omega > \omega_0 - \delta$ . Despite this complication  $\langle\beta\rangle$  and  $\beta_{\max}$  can be well-defined over the entire domain of  $\omega$ : they represent, respectively, the average and the maximum  $\beta$  over all possible directions of  $\mathbf{k}$ . The plots of these functions for  $\omega > \omega_0 - \delta$  depend on the shape of the canonical FR which is determined by the symmetry. Example plots of  $\langle\beta\rangle$  and  $\beta_{\max}$  versus  $\omega$  for the cubic symmetry  $m\bar{3}m$  (for which  $\omega_0 = \pi/4$ ) are shown in Fig. 6. Data for the plots were obtained numerically: Orientation having a given  $\omega$  and random  $\mathbf{k}$ , and located in FR was generated, it was perturbed by a rotation error with fixed angle  $\delta$  and random axis, the perturbed orientation was represented in FR, the vector  $\mathbf{k}'$  along the axis was determined, and the angle  $\beta$  between  $\mathbf{k}$  and  $\mathbf{k}'$  was computed. For a given  $\omega$ , these steps were repeated  $10^5$  and  $10^6$  times to get  $\langle\beta\rangle$  and  $\beta_{\max}$ , respectively.

Summarizing, if the angle  $\omega + \delta$  is smaller than  $\omega_0$ , formulas of section 3 are applicable. If a rotation representing an orientation in FR is close to the boundary of the region, one needs to take into consideration representations outside the region.

### *Misorientations*

As in the case of orientations, one can construct an FR for misorientations, but unlike with orientations, there are no canonical conditions that make it unique. The  $I$ -based Voronoi cell cannot be used because there are a number of equivalent points at exactly the same distance from  $I$ .<sup>3</sup> If the average of  $\beta$  were calculated based on points in FR, the result would depend on the choice of the region and would vary from case to case.

Hence it follows that without a priori knowledge enabling the selection of a specific frame from among equivalent crystal reference frames, the approach applicable to orientations (i.e., averaging over data in FRs) and figures analogous to Fig. 6 are of no practical significance in the case of misorientations, and the subject of the average error in determination of misorientation axis is not resolved by expressions of the type (1) and (2). Therefore, when encountering the average error in determining the misorientation axis, one should be aware that the special case is considered in which reference systems are selected a priori and crystal symmetry does not play any role.

---

<sup>3</sup>An additional complication is the grain exchange symmetry which arises when crystallites are not distinguished. With the axis/angle parameterization, the grain exchange symmetry comes down to the equivalence of  $(\mathbf{k}, \omega)$  and  $(-\mathbf{k}, \omega)$ . This symmetry is usually assumed in analyses of EBSD orientation maps.

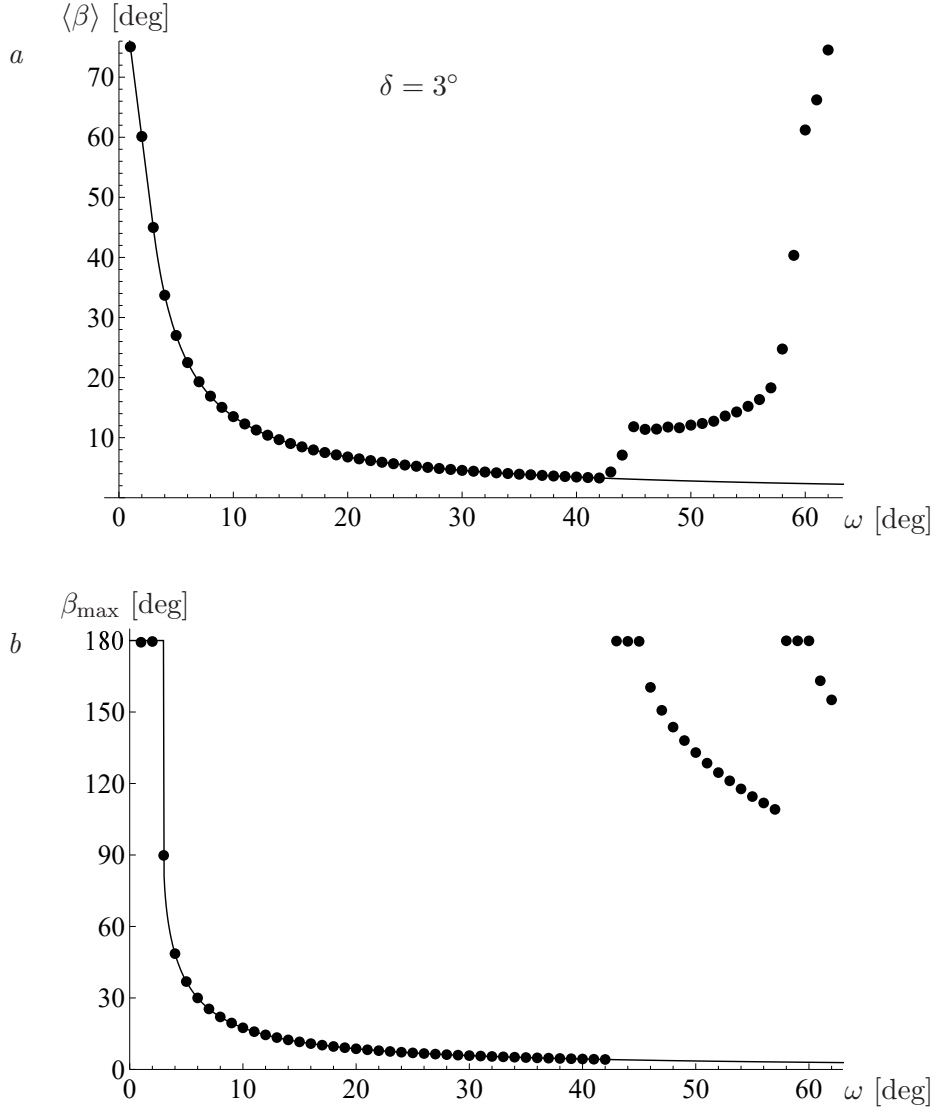


Figure 6: The average angle  $\langle\beta\rangle$  (a) and the maximal angle  $\beta_{\max}$  (b) between axes of the actual and an error-affected orientations versus rotation angle  $\omega$  for the errors of magnitude  $\delta = 3^\circ$  and cubic crystal symmetry (disks). The continuous curves correspond to  $\langle\beta\rangle$  and  $\beta_{\max}$  shown in Fig. 2. Unlike the case illustrated in Fig. 3, where  $\beta_{\max} = \pi$  for  $\omega > \pi - \delta$ , here the angle  $\beta_{\max}$  can be smaller than  $\pi$  for  $\omega > \omega_0 - \delta$ . The reason is that, generally, axis of a rotation located just outside the boundary of FR is not opposite to the axis of its equivalent in FR. This also affects the dependence of  $\langle\beta\rangle$  on  $\omega$  in the range  $\omega > \omega_0 - \delta$ .

## 6 Concluding remarks

Axes of rotations together with rotation angles are the basic means of describing orientations and misorientations of crystals. Rotation axes are also a tool for studying some properties of crystalline materials. Crystal orientations are usually determined with some errors, and the question is how this affects rotation axes obtained from such data.

With  $\beta$  denoting the angle between axes of the actual rotation and its approximation, the average  $\langle\beta\rangle$  and the maximal  $\beta_{\max}$  are convenient measures of the uncertainty of the rotation axes. The paper addresses the formal issue of determining  $\langle\beta\rangle$  and  $\beta_{\max}$  when rotation data are affected by random errors of fixed magnitude. Analytical formulas for  $\langle\beta\rangle$  and  $\beta_{\max}$  as functions of the rotation angle and the error magnitude are provided. Additionally, a method for estimating the average of  $\beta$  in the practical case of rotation errors following the von Mises-Fisher distribution is described. These solutions are applicable in texture-related calculations to estimate the reliability of rotation axes. In particular, they are crucial to assessing the accuracy of axes of small-angle misorientations, which are of interest in connection with the determination of Taylor axes and slip systems.

For data obtained from crystalline materials, an additional factor is the crystal symmetry. It can be ignored only if there are preconditions enabling selection of a specific reference frame from among equivalent frames. Otherwise, to avoid ambiguities, data are reduced to fundamental regions. In the case of orientations, there is a canonical fundamental region which consists of minimum-angle rotations, and the average and maximal  $\beta$  over data in this region are well defined. There is no canonical choice of the fundamental region for misorientations, and therefore there are no simple definitions of the average or maximal  $\beta$ .

## Appendix A

**The angles  $\langle\beta\rangle$  and  $\beta_{\max}$  for  $0 < \omega \leq \pi$**

To simplify comparisons with the work of Bate et al. [9], most of their notation is retained. The expression (A4) of [9] for the angle  $\beta$  (between axes of the actual and error affected rotations) can be written as

$$\beta(\mathbf{h}) = \arccos \left( \frac{\cos(\delta/2) \sin(\omega/2) + \sin(\delta/2) \cos(\omega/2) (\mathbf{k} \cdot \mathbf{h})}{\sqrt{1 - (\cos(\delta/2) \cos(\omega/2) - \sin(\delta/2) \sin(\omega/2) (\mathbf{k} \cdot \mathbf{h}))^2}} \right), \quad (5)$$

where  $\mathbf{k}$  and  $\mathbf{h}$  are unit vectors along axes of the rotation  $g$  and the error rotation  $g'g^{-1}$ , respectively. Formula (5) does not account for the case with  $\omega$  exceeding  $\pi - \delta$ , i.e., when the error affected rotation is close to a half-turn. At the half-turn, the error affected rotation switches the axis direction. To take this into account, one needs to include the index  $c_s(\mathbf{h}) = \text{sgn}(\cos(\delta/2) \cos(\omega/2) - \sin(\delta/2) \sin(\omega/2) (\mathbf{k} \cdot \mathbf{h}))$  as a factor in front of the argument of arccos in eq.(5). This coefficient results from consistent application of formulas for composition of rotations and definition of the rotation axis.

Due to the homogeneity of the space of rotations, the dependence of  $\beta$  on  $\mathbf{h}$  can be explored with any  $\mathbf{k}$ ; this can be the unit vector along the  $z$  axis of the Cartesian coordinate system. With  $\mathbf{h}$  specified by spherical coordinates  $\theta$  (polar angle) and  $\phi$  (azimuthal angle), one has  $\mathbf{k} \cdot \mathbf{h} = \cos \theta$ . Thus, for given  $\delta$  and  $\omega$ , the angle  $\beta$  depends only on  $\theta$

$$\beta(\theta) = \arccos \left( c_s(\theta) \frac{\cos(\delta/2) \sin(\omega/2) + \sin(\delta/2) \cos(\omega/2) \cos \theta}{\sqrt{1 - (\cos(\delta/2) \cos(\omega/2) - \sin(\delta/2) \sin(\omega/2) \cos \theta)^2}} \right). \quad (6)$$

With random distribution of  $\mathbf{h}$ , the average of  $\beta$  is given by the integral over the unit sphere  $S^2$

$$\langle\beta\rangle = \int_{S^2} \beta(\mathbf{h}) d\mathbf{h} = \frac{1}{4\pi} \int_{S^2} \beta(\theta) \sin \theta d\theta d\phi = \frac{1}{2} \int_0^\pi \beta(\theta) \sin \theta d\theta.$$

The integration can be carried out using software for symbolic computation. Let

$$\xi_1^\pm(\omega, \delta) = 1 \pm \cos(\delta/2) \cos(\omega/2) \quad \text{and}$$

$$\xi_2^\pm(\omega, \delta) = \pi - 2 \arccos(\sin(\delta/2) \sin(\omega/2) \mp \xi_1^\pm(\omega, \delta) \cot(\delta/2) \cot(\omega/2)),$$

where either lower or upper sign is used concurrently on both sides. For  $0 < \omega < \pi - \delta$  the dependence of the average of  $\beta$  on  $\omega$  and  $\delta$  is

$$\langle\beta\rangle(\omega, \delta) = \frac{1}{2} \arccos(\text{sgn}(\omega - \delta)) + \frac{\pi}{4} \frac{\text{sgn}(\omega - \delta) \xi_1^-(\omega, \delta) + \xi_1^+(\omega, \delta) - 2 \cos(\delta/2)}{\sin(\delta/2) \sin(\omega/2)}, \quad (7)$$

and if  $\omega \geq \pi - \delta$ , then

$$\langle\beta\rangle(\omega, \delta) = \frac{1}{2} \arccos(\text{sgn}(\omega - \delta)) + \xi_3(\omega, \delta) + \xi_4(\omega, \delta) - \text{sgn}(\omega - \delta) \xi_5^-(\omega, \delta) + \xi_5^+(\omega, \delta), \quad (8)$$

where

$$\begin{aligned}\xi_3(\omega, \delta) &= \frac{\pi}{2} - \frac{\cot(\delta/2)}{\sin(\omega/2)} \arcsin(\cot(\delta/2) \cot(\omega/2)) , \\ \xi_4(\omega, \delta) &= \frac{1}{2} \left( \arccos\left(\frac{\cos(\delta/2)}{\sin(\omega/2)}\right) - \arccos\left(-\frac{\cos(\delta/2)}{\sin(\omega/2)}\right) \right) \cot(\delta/2) \cot(\omega/2) , \\ \xi_5^\pm(\omega, \delta) &= \frac{\xi_1^\pm(\omega, \delta) \xi_2^\pm(\omega, \delta)}{4 \sin(\delta/2) \sin(\omega/2)} .\end{aligned}$$

If  $\omega > \delta$ , then eq.(7) reduces to simple eq.(1).

It is easy to get the maximal deviation  $\beta_{\max}$ . With  $\delta < \omega < \pi - \delta$ , the condition  $d\beta/d\theta = 0$  for extrema of  $\beta(\theta)$  is satisfied if

$$\sin \theta = 0 \quad \text{or} \quad \sin \delta \sin(\omega/2) \cos \theta + 2 \sin^2(\delta/2) \cos(\omega/2) = 0 .$$

The maximum of  $\beta$  corresponds to the second case, i.e., to  $\cos \theta = -\tan(\delta/2) \cot(\omega/2)$ . Substitution of this  $\cos \theta$  into (6) gives

$$\beta_{\max}(\omega, \delta) = \arccos\left(\sqrt{\frac{\cos \delta - \cos \omega}{1 - \cos \omega}}\right) .$$

If  $\omega \leq \delta$  or  $\omega \geq \pi - \delta$ , the rotation affected by random error of magnitude  $\delta$  may have any axis, so  $\beta_{\max} = \pi$ .

## Appendix B

### Distribution of magnitudes of 'random' error rotations

Random measurement errors of physical quantities represented by real-valued variables are often assumed to have normal distributions. However, the Gaussian distribution is not suitable for orientation data. For such data, a convenient analogue of the (trivariate) normal distribution is the function described by the von Mises-Fisher distribution for special orthogonal matrices; see, e.g., [25, 26].

The simplest of the von Mises-Fisher type distributions are unimodal with 'spherical' symmetry, i.e. they depend only on the angular distance  $\delta$  between the variable and the mean and are independent of the axis of rotation relating these two points. They are of the form  $c(\kappa) \exp(\kappa \cos \delta)$  [25]. The invariant volume element on the space of rotations in axis ( $\mathbf{h}$ ) and angle ( $\delta$ ) parameterization is  $(2/\pi) \sin^2(\delta/2) d\delta d\mathbf{h}$  [31]. Thus, with a unimodal 'spherical' von Mises-Fisher orientation distribution, the distribution  $p$  of the angles  $\delta$  is proportional to  $\sin^2(\delta/2) \exp(\kappa \cos \delta)$ . After normalization to 1, it can be expressed as

$$p(\delta, \hat{\delta}) = N(\hat{\delta}) q(\delta, \hat{\delta}) \exp\left(-q(\delta, \hat{\delta})\right) ,$$

where

$$q(\delta, \hat{\delta}) = \left(\frac{\sin(\delta/2)}{\sin(\hat{\delta}/2)}\right)^2 ,$$

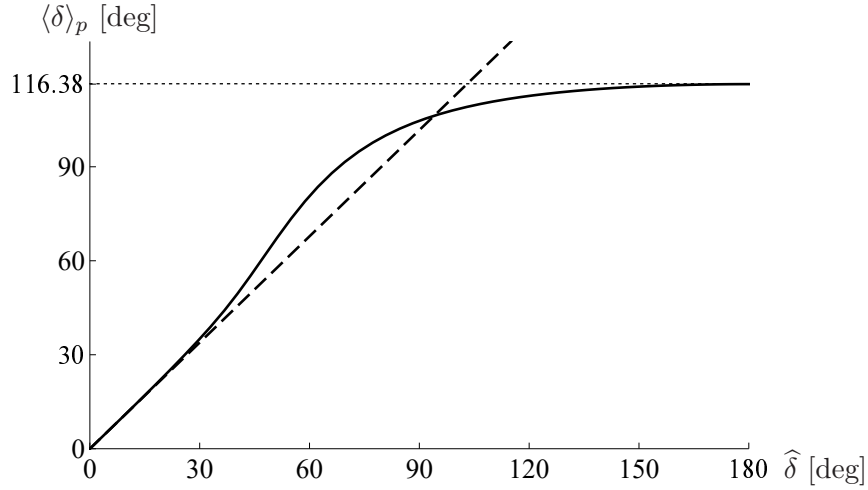


Figure 7: The average  $\langle \delta \rangle_p = \int_0^\pi \delta p(\delta, \hat{\delta}) d\delta$  versus  $\hat{\delta}$  for  $p$  given by (3). The dashed line (tangent to the solid line at  $0^\circ$ ) is described by  $\langle \delta \rangle_p = 1.13 \hat{\delta}$ .

the normalization coefficient is

$$N(\hat{\delta}) = \frac{1}{Q(\csc^2(\hat{\delta}/2)/2)},$$

the function  $Q$  is given by

$$Q(\kappa) = \pi \kappa e^{-\kappa} (I_0(\kappa) - I_1(\kappa)),$$

and  $I_n$  is the modified Bessel function of the first kind and order  $n$ . The distribution  $p$  can be specified using the location of its maximum  $\hat{\delta}$  ( $0 < \hat{\delta} \leq \pi$ ) or the average  $\langle \delta \rangle_p = \int_0^\pi \delta p(\delta, \hat{\delta}) d\delta$ . The numerically determined one-to-one relationship of  $\langle \delta \rangle_p$  to  $\hat{\delta}$  is shown in Fig. 7.

## References

- [1] D.J. Prior. Problems in determining the misorientation axes, for small angular misorientations, using electron backscatter diffraction in the SEM. *J. Microsc.*, 195:217–225, 1999.
- [2] I. Cross and V. Randle. Lowest angle solution versus low-index axis solution for misorientations. *Scripta Mater.*, 48:1587–1591, 2003.
- [3] S.M. Reddy and C. Buchan. Constraining kinematic rotation axes in high-strain zones: a potential microstructural method? *Geological Society, London, Special Publications*, 243:1–10, 2005.
- [4] Y.B. Chun, M. Battaini, C.H.J. Davies, and S.K. Hwang. Distribution characteristics of in-grain misorientation axes in cold-rolled commercially pure titanium and their correlation with active slip modes. *Metall. Mater. Trans. A*, 41:3473–3487, 2010.
- [5] M. Yamasaki, K. Hagihara, S. Inoue, J.P. Hadorn, and Y. Kawamura. Crystallographic classification of kink bands in an extruded Mg–Zn–Y alloy using intragranular misorientation axis analysis. *Acta Mater.*, 61:2065–2076, 2013.
- [6] R. Jeyaraam, S. Vedantam, and V.S. Sarma. On the significance of misorientation axes of CSL boundaries in triple junctions in cubic materials. *Mater. Char.*, 152:276–281, 2019.
- [7] C. Li, J. Sun, A. Feng, H. Wang, X. Zhang, C. Zhang, F. Zhao, G. Cao, S. Qu, and D. Chen. Active slip mode analysis of an additively manufactured Ti-6Al-4V alloy via in-grain misorientation axis distribution. *Metals*, 12:532, 2022.
- [8] A. Godfrey, G.L. Wu, and Q. Liu. Characterisation of orientation noise during EBSP investigation of deformed samples. In *Textures of Materials - ICOTOM 13*, volume 408 of *Mater. Sci. Forum*, pages 221–226, 2002.
- [9] P.S. Bate, R.D. Knutsen, I. Brough, and F.J. Humphreys. The characterization of low-angle boundaries by EBSD. *J. Microsc.*, 220:36–46, 2005.
- [10] A. Morawiec, E. Bouzy, H. Paul, and J.J. Fundenberger. Orientation precision of TEM-based orientation mapping techniques. *Ultramicroscopy*, 136:107–118, 2014.
- [11] J. Stuelpnagel. On the parametrization of the three-dimensional rotation group. *SIAM Rev.*, 6:422–430, 1964.
- [12] A.J. Wilkinson, G. Meaden, and D.J. Dingley. High resolution mapping of strains and rotations using electron backscatter diffraction. *Mater. Sci. Technol.*, 22:1271–1278, 2006.

- [13] I. Brough, P.S. Bate, and F.J. Humphreys. Optimising the angular resolution of EBSD. *Mater. Sci. Technol.*, 22:1279–1286, 2006.
- [14] F.J. Humphreys and P.S. Bate. The microstructures of polycrystalline Al–0.1 Mg after hot plane strain compression. *Acta Mater.*, 55:5630–5645, 2007.
- [15] M.U. Farooq, R. Villaurrutia, I. MacLaren, H. Kungl, M.J. Hoffmann, J.J. Fundenberger, and E. Bouzy. Using EBSD and TEM-Kikuchi patterns to study local crystallography at the domain boundaries of lead zirconate titanate. *J. Microsc.*, 230:445–454, 2008.
- [16] R. Quey, D. Piot, and J.H. Driver. Microtexture tracking in hot-deformed polycrystalline aluminium: Experimental results. *Acta Mater.*, 58:1629–1642, 2010.
- [17] A.J. Wilkinson and D. Randman. Determination of elastic strain fields and geometrically necessary dislocation distributions near nanoindents using electron back scatter diffraction. *Philos. Mag.*, 90:1159–1177, 2010.
- [18] C.J. Gardner, J. Kacher, J. Basinger, B.L. Adams, M.S. Oztop, and J.W. Kysar. Techniques and applications of the simulated pattern adaptation of Wilkinson’s method for advanced microstructure analysis and characterization of plastic deformation. *Exp. Mech.*, 51:1379–1393, 2011.
- [19] F. Ram, S. Zaefferer, T. Jäpel, and D. Raabe. Error analysis of the crystal orientations and disorientations obtained by the classical electron backscatter diffraction technique. *J. Appl. Cryst.*, 48:797–813, 2015.
- [20] A. Albou. *Influence de l’orientation cristalline sur les microstructures de déformation et l’adoucissement d’alliages Al-Mn*. PhD thesis, Ecole Nationale Supérieure des Mines de Saint-Etienne, 2010.
- [21] L. Renversade. *Experimental and numerical analysis of single grain plasticity in an aluminium polycrystal deformed in uniaxial tension*. PhD thesis, Université de Lyon, 2016.
- [22] H. Qu. *Understanding mechanistic effect of chloride-induced stress corrosion cracking mechanism through multi-scale characterization*. PhD thesis, Purdue University Graduate School, 2023.
- [23] A.J. Wilkinson. A new method for determining small misorientations from electron back scatter diffraction patterns. *Scr. Mater.*, 44:2379–2385, 2001.
- [24] V. Tong, H. Jones, and K. Mingard. Micropillar compression of single crystal tungsten carbide, Part 2: Lattice rotation axis to identify deformation slip mechanisms. *Int. J. Refract. Met. H.*, 103:105734, 2022.

- [25] C.G. Khatri and K.V. Mardia. The von Mises-Fisher matrix distribution in orientation statistics. *J. R. Stat. Soc. B*, 39:95–106, 1977.
- [26] M.J. Prentice. Orientation statistics without parametric assumptions. *J. R. Statist. Soc. B*, 48:214–222, 1986.
- [27] T. Yeates. The asymmetric regions of rotation functions between Patterson functions of arbitrarily high symmetry. *Acta Cryst. A*, 49:138–141, 1993.
- [28] A. Morawiec. Distributions of misorientation angles and misorientation axes for crystallites with different symmetries. *Acta Cryst. A*, 53:273–285, 1997.
- [29] A. Morawiec. *Orientations and Rotations. Computations in Crystallographic Textures*. Springer–Verlag, Berlin, 2004.
- [30] R. Krakow, R.J. Bennett, D.N. Johnstone, Z. Vukmanovic, W. Solano-Alvarez, S.J. Lainé, J.F. Einsle, P.A. Midgley, C.M.F. Rae, and R. Hielscher. On three-dimensional misorientation spaces. *Proc. Roy. Soc. A*, 473:20170274, 2017.
- [31] R.E. Miles. On random rotations in  $R^3$ . *Biometrika*, 52:636–639, 1965.